Anal Bioanal Chem (2005) 381: 788–794
DOI 10.1007/s00216-004-2918-1

ORIGINAL PAPER

Edwin A. Hernández-Caraballo · Francklin Rivas
Rita M. Ávila de Hernández

Evaluation of a generalized regression artificial neural network for extending cadmium's working calibration range in graphite furnace atomic absorption spectrometry

Received: 25 August 2004 / Revised: 12 October 2004 / Accepted: 14 October 2004 / Published online: 2 February 2005

Abstract A generalized regression artificial neural network (GRANN) was developed and evaluated for modeling cadmium's nonlinear calibration curve in order to extend its upper concentration limit from 4.0 μg L^{-1} up to 22.0 μg L^{-1}. This type of neural network presents important advantages over the more popular backpropagation counterpart which are worth exploiting in analytical applications, namely, (1) a smaller number of variables have to be optimized, with the subsequent reduction in "development hassle"; and, (2) shorter development times, thanks to the fact that the adjustment of the weights (the artificial synapses) is a non-iterative, one-pass process. A backpropagation artificial neural network (BPANN), a second-order polynomial, and some less frequently employed polynomial and exponential functions (e.g., Gaussian, Lorentzian, and Boltzmann), were also evaluated for comparison purposes. The quality of the fit of the various models, assessed by calculating the root mean square of the percentage deviations, was as follows: GRANN > Boltzmann > second-order polynomial > BPANN > Gauss > Lorentz. The accuracy and precision of the models were further estimated through the determination of cadmium in the certified reference material "Trace Metals in Drinking Water" (High Purity Standards, Lot No. 490915), which has a cadmium certified concentration (12.00 ± 0.06 μg L^{-1}) that lies in the nonlinear regime of the calibration curve. Only the models generated by the GRANN and BPANN accurately predicted the concentrations of a series of solutions, prepared by serial dilution of the CRM, with cadmium concentrations below and above the maximum linear calibration limit (4.0 μg L^{-1}). Extension of the working range by using the proposed methodology represents an attractive alternative from the analytical point of view, since it results in less specimen manipulation and consequently reduced contamination risks without compromising either the accuracy or the precision of the analyses. The implementation of artificial neural networks also helps to reduce the trial-and-error task of looking for the right mathematical model from among the many possibilities currently available in the various scientific and statistic software packages.

Keywords Cadmium · Graphite furnace atomic absorption spectrometry (GFAAS) · Calibration curve · Modeling · Artificial neural networks

E. A. Hernández-Caraballo (✉) · F. Rivas
R. M. Ávila de Hernández
Laboratorio de Sistemas Inteligentes,
Escuela de Ingeniería de Sistemas,
Facultad de Ingeniería, Universidad de Los Andes,
Merida, 5101-A, Venezuela
E-mail: ea_hernandezc@yahoo.com

R. M. Ávila de Hernández
Departamento de Procesos Agroindustriales,
Programa de Ingeniería Agroindustrial,
Decanato de Agronomía,
Universidad Centro-Occidental Lisandro Alvarado,
Núcleo Obelisco, Barquisimeto, 3002, Venezuela

Introduction

Graphite furnace atomic absorption spectrometry (GFAAS) has an established niche in the analyst's arsenal as a powerful technique for the determination of atomic species at trace concentrations. Nevertheless, it suffers from various disadvantages, one of them being its short linear dynamic range [1]: this may represent an important issue if the concentration of an analyte in a given sample exceeds the upper concentration limit on the calibration curve. Under such circumstance the analyst may be forced to dilute the laboratory solution, with the ensuing risk of contamination and, inevitably, increasing the preparation time and the analysis costs. In order to cope with the aforementioned handicap, several analytical, instrumental, and mathematical approaches

have been proposed [2]. With regards to the last of these, which is actually the focus of the present work, three different strategies may be highlighted: (1) linearization of the calibration curve by correcting for the cause of its ''bending'' [3]; (2) modeling the nonlinear calibration curve [4]; and, less frequently, (3) a combination of both approaches [2].

Modeling the nonlinear calibration curves is usually carried out by means of second- or third-order polynomial fittings [4]. Another interesting yet overlooked alternative may be modeling by means of artificial neural networks (ANNs) [5–8]. ANNs trained with the ''backpropagation'' algorithm, commonly referred to as backpropagation artificial neural networks (BPANNs), are certainly the most popular among analytical applications [9]. Nonetheless, such ANNs are not devoid of problems, among which the long development times are one. Based on the above observation, we decided to evaluate another approach based on a scarcely known kind of ANN, namely, the generalized regression ANN (GRANN): this is a variation of the radial basis ANN which can be used as a ''soft'' approximation to unknown or complex mathematical functions [10]. The most attractive feature of this kind of network is that its development time is significantly shorter than the analogous process with the backpropagation counterpart. Training in this case is a ''one-pass'' step in which no weight-adjustment iteration process is required. Such an advantage, along with the nonlinear modeling capabilities characteristic of an ANN, should make of this an appealing alternative to other common and uncommon modeling techniques. As far as the authors are aware, the GRANN has never been used for modeling purposes in spectrochemical analysis. Cadmium was selected as the model analyte owing to its short linear dynamic range. The results obtained by means of the GRANN were compared to those obtained after fitting the calibration curve with other mathematical functions, namely, a second-order polynomial, some exponential functions (Gaussian, Boltzmann, and Lorentzian fits) [7], as well as with the results obtained with a previously developed BPANN [8].

Experimental

Equipment, accessories, and software

A Perkin–Elmer atomic absorption spectrometer, model 2100, equipped with an electrothermal atomization system model HGA-700, an autosampler system model AS-70, and a deuterium lamp background correction system was used. Pyrolytically coated graphite atomizers (Perkin–Elmer) with totally pyrolytic graphite platforms (Perkin–Elmer) were employed after proper conditioning [11]. A monoelemental, cadmium hollow-cathode lamp (Varian), operated at 6 mA, was used at the 228.8-nm Cd line. All other conditions were as recommended by the spectrometer manufacturer.

The GRANN was developed in Matlab (The Mathworks, Inc., MA, USA) by means of the Neural Network Toolbox [10]. Mathematical fitting of the data with the polynomial and exponential functions was performed with Microcal Origin 6.0 (Microcal Software, Inc., MA, USA).

Reagents and materials

Cadmium metal powder (Merck, pro analysi) was employed for preparation of the analyte's stock solution. Ten percent (10% w/v) palladium nitrate solution (Aldrich) and magnesium nitrate hexahydrate (Carlo Erba) were used as chemical modifiers. Nitric acid (Alfa Aesar, metal basis, 99.999% purity) served for dilution and stabilization of solutions. Distilled, de-ionized water (Millipore, 18 $M\Omega\ cm^{-1}$) was utilized for preparation of sample and standard solutions.

The certified reference material ''Trace Metals in Drinking Water'' (High Purity Standards, Lot No. 490915) was employed to verify the accuracy of the methodology hereby proposed. This reference material has a certified concentration of cadmium of $12.00 \pm 0.06\ \mu g\ L^{-1}$ [12].

Procedure

Preparation of working solutions

Cadmium standards were prepared from a laboratory-made stock solution (1,000 mg L^{-1} Cd in 1.0% HNO_3) by dilutions with a 0.2% v/v HNO_3 solution. Fifteen standard solutions were prepared so as to yield working solutions with cadmium concentrations spanning from 0 (blank) to 22.0 μg L^{-1} Cd. A 6,000 mg L^{-1} magnesium nitrate solution was prepared by weighing an exact amount (1.037 g) of $Mg(NO_3)_2.\ 6H_2O$ and diluting to 100 mL with 0.2% v/v HNO_3. A mixed 500 mg L^{-1} Pd + 300 mg L^{-1} $Mg(NO_3)_2$ chemical modifier was prepared directly in an autosampler vial by dilution of the corresponding solutions. Various solutions of the certified reference material were prepared to yield cadmium concentrations at four levels so that two of them were inside and the other two outside the linear calibration range.

Determination of cadmium by GFAAS

The conditions for the determination of cadmium by GFAAS have been previously optimized [8]. Briefly, 10 μL of the standards/samples, and 10 μL of a mixed chemical modifier consisting of 5 μg Pd + 3 μg $Mg(NO_3)_2$ were injected sequentially into a pre-heated graphite furnace electrothermal atomizer (injection temperature 100°C; injection rate 40%), and the atomization program shown in Table 1 was run. The chemi-

Table 1 Atomization program for the determination of Cd by GFAAS

Step	Temperature (°C)	Ramp (s)	Hold (s)
Dry	200	20	5
Pyrolysis	800	5	15
Cool down I	50	1	5
Cool down II[a]	50	1	5
Atomization[a]	1,400	0	3 (Read)
Clean	2,500	1	3
Cool down	20	1	8

All temperatures reported are nominal
[a]Gas stop mode; 300 mL min^{-1} Ar flow in all other stages

cal modifier was employed to improve cadmium's peak profile, as running the certified reference material in its absence resulted in the appearance of a distorted analytical signal. The reason for such a distortion, presumably the result of the high concentration of certain elements (e.g., sodium and calcium [12]), was not investigated, but it was satisfactory corrected for by the addition of the aforementioned modifier. Five replicates (integrated absorbance values) for each standard/sample were taken. Replicate runs of the calibration standards resulted in a database comprising 75 patterns, i.e., integrated absorbance–concentration data pairs, which were randomly sorted into training and validation subsets. These subsets were employed in the development and evaluation of the various mathematical and neural network models, respectively.

Artificial neural networks

A backpropagation and a GRANN were evaluated in the present work. Both shared a common feature, namely, a two-layer structure, but differ in many other respects. The underlying principles of the backpropagation ANNs have been amply described elsewhere (see for example ref. [13]), and therefore they will not be dealt with here. The BPANN employed herein was developed and evaluated in a previous work [8]. Basically, it comprises an input node, two hidden neurons with sigmoid transfer functions, and a single output neuron with a linear transfer function. The user introduces the integrated absorbance value for a given solution and the network predicts the corresponding concentration. The network was trained for 10^5 cycles by using the generalized delta rule as the training algorithm and the reduction of the mean square error (MSE) as the optimization criteria [14]. The learning rate (λ) and the momentum factor (μ) were empirically adjusted to 0.04 and 0.4, respectively, to yield the lowest MSE.

A generalized regression ANN is a variation of the radial basis ANN that is based on the Nadaraya–Watson kernel regression [15, 16]. It is comprised of two active layers, both of which have as many neurons as training patterns. The neurons on the first (hidden) layer of all radial basis ANNs process the input data by means of a radial basis function (hence the name):

$$\mathrm{RBF} = \exp\left(-\frac{(\|c_i - p_i\|b)^2}{\sigma_I}\right) \quad (1)$$

where c_I, σ_I are the centroids and width of the I-th radial basis function, respectively; p_I is the I-th value of the input vector, and b is the bias. The latter is in turn estimated according to (0.8326/SPREAD) [10], whereby SPREAD is a non-zero, positive real number. The second (output) layer has a linear transfer function. The weights of the output neurons are initially set to the desired output values (keep in mind that training the BPANN and the GRANN is a supervised process). The overall GRANN output is a weighted average of the target values of the training cases close to a given input case. When an input vector is very close to any of the training patterns (i.e., $|c_I - p_I| \approx 0$ in Eq. 1), the first layer output will be ≈ 1, and the second layer will give an output very close to the matching training output. The train and prediction subsets were the same ones employed in the development and evaluation of the backpropagation ANNs. No validation group was required in this case.

Forty five integrated absorbance-normalized concentration pairs (60% of the entire calibration data set), covering the entire working calibration range, were randomly selected in order to develop both the BPANN and the GRANN; the remaining 30 patterns (40% of the calibration data set) were used in evaluating the performance of the models thus generated. The use of normalized concentrations instead of raw concentrations was the result of a preliminary assessment which revealed that lower mean squared errors were achieved with such transformation of the data [8].

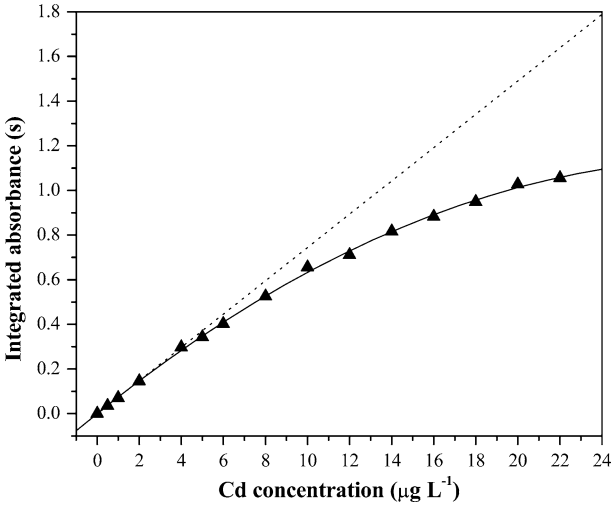

Fig. 1 Cadmium's working calibration curve (*solid line*). The linear calibration equation has been purposely extended throughout the entire working range (*dotted line*) for comparison purposes

Evaluating the model performance

The prediction ability of the models tested in the present work was assessed by three different means. First, by computing the root mean square of the percentage deviations (RMSPD) [17]:

$$\mathrm{RMSPD} = \left(\frac{1}{N} \sum_{I=1}^{N} \left(\frac{C^{I}_{\mathrm{Pred}} - C^{I}_{\mathrm{Real}}}{C^{I}_{\mathrm{Real}}} \times 100 \right)^{2} \right)^{\frac{1}{2}} \quad (2)$$

where C^{I}_{Pred} and C^{I}_{Real} correspond to the I-th predicted and actual concentrations, respectively; N is the number of points used in the calibration (excluding the blank). Second, by evaluating the quality of the linear regression analyses that resulted from plotting the predicted concentrations for each one of the models versus the nominal concentrations of the standards solutions along the entire working range. Finally, through the determination of the concentration of cadmium in the solutions prepared from the certified reference material.

Results and discussions

Cadmium calibration curve in GFAAS

Figure 1 shows the trend in cadmium's integrated absorbance signal with increasing concentrations. Above the maximum concentration value depicted in Fig. 1 (22.0 μg L^{-1} Cd) the curve reached a quasi-plateau, and so those X–Y pairs were discarded from the studies that followed. The linear relationship between integrated absorbance (A_I) and cadmium concentration, best described by the equation $A_I = 0.0745[\mathrm{Cd}]_I - 0.0019$ ($r^2 = 0.9998$), spanned only up to 4.0 μg L^{-1}. The dotted lines in Fig. 1 correspond to the extrapolation of the integrated absorbance along the entire working concentration range, and it serves to highlight how strongly the response variable deviates from the much appreciated linearity. Such a short linear range entails that those test solutions having concentrations higher than the upper limit would require dilution, with all the disadvantages already mentioned. An alternative approach to minimizing such problems could be modeling the nonlinear calibration curve so as to extend the working range.

Modeling the nonlinear calibration curve

A series of mathematical equations along with two ANNs were evaluated for modeling the working calibration curve. Some of the mathematical functions, namely, Lorentzian, Gaussian, and Boltzmann fits, were selected following a work by Sun et al. [7], based on their successful application in modeling a nonlinear spectrophotometric calibration curve. The second-order polynomial is an option that is certainly more common than the aforementioned ones [4], and was thus also chosen for evaluation.

The following equations were found to fit the experimental data:

– Second-order polynomial:

$$A_i = 0.0002 + 0.0758[\mathrm{Cd}]_I - 0.0012[\mathrm{Cd}]_I^2 \quad (3)$$

– Lorentzian:

$$A_i = -2.598 + \frac{20445.533}{4 \cdot \left([\mathrm{Cd}]_I - 23.470\right)^2 + 5612.384} \quad (4)$$

– Gaussian:

$$A_i = -2.577 + 3.654 \cdot \exp\left[\frac{-2 \cdot \left([\mathrm{Cd}]_I - 25.874\right)^2}{(62.201)^2} \right] \quad (5)$$

– Boltzmann:

$$A_i = \frac{-4.523}{\left[1 + \exp\left(\frac{[\mathrm{Cd}]_I + 10.244}{12.540}\right)\right]} + 1.384 \quad (6)$$

It is worth mentioning at this point that we are aware that some workers may argue against the use of such calibration functions due to their lack of physical meaning. However, we persist in our position that as long as they serve their purpose with an acceptable degree of accuracy and precision then they should not be disregarded as alternative calibration techniques [8]. Clearly, it is possible to find many more possible equations in almost any scientific software. The various software packages developed by the firms dealing with the manufacture of current spectrometers also have a built-in algorithm for modeling the calibration function. However, the problem still remains in that selecting an adequate mathematical function and adjusting the corresponding coefficients to yield the highest goodness-of-fit is not an easy task even with current scientific software. This is the reason why ANNs are so appealing when it comes to modeling non-linear processes in general. With these tools, it is not necessary to invest the analyst time in what Bysouth and Tyson [18] referred to as "the non-productive part" of the analysis.

The backpropagation ANN was selected on the basis of its popularity [9] and on its successful implementation in a previous work [8]. The GRANN, quite contrarily, has been scarcely evaluated for modeling purposes [19–21]. This variety of ANN presents various attractive features. Effectively, in the first place, the number of neurons in both active layers is automatically determined by the number of patterns selected by the user for training the network. Second, only the width of the radial basis function has to be selected during the optimization process. In contrast, developing a BPANN implies adjusting several variables, namely, learning rate, momentum factor, number of hidden neurons, and training cycles, as well as assessing the most adequate

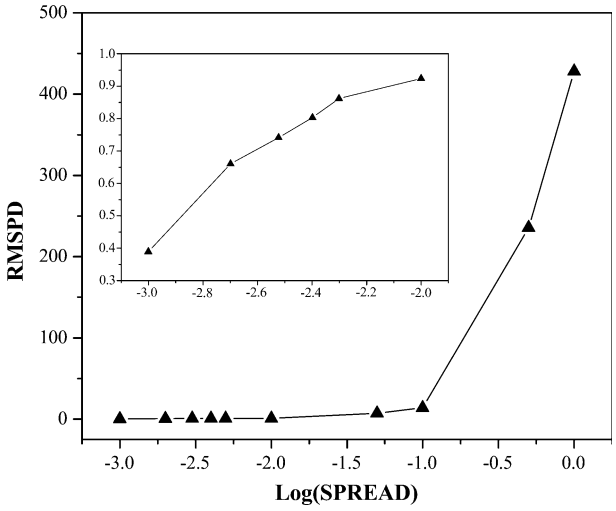

Fig. 2 Variation of the RMSPD as a function of the logarithm of the SPREAD value for optimization of the GRANN. *Inset* shows the detailed behavior of the RMSPD when the SPREAD value was varied between 1×10^{-3} and 1×10^{-2}

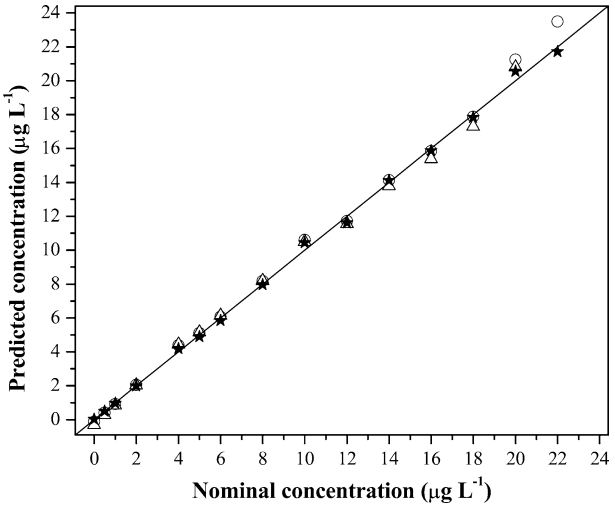

Fig. 3 Predicted versus nominal cadmium concentrations for the Lorentzian (*triangles*),Gaussian (*circles*), and Boltzmann (*stars*) models. The *solid line* represents the perfect correlation between the two variables

transfer functions for the hidden and output layers. One final aspect that also exerts a huge impact on the overall development process is that training a GRANN, in opposition to a BPANN, is a non-iterative, one-pass process. In this context, while it took 15–27 s for a Pentium III processor to complete 8×10^4 iterations when training one of the many possible topologies for a BPANN [8], the task of developing the one and only GRANN required to model the calibration curve was completed in a fraction of a second. Although the time taken by a BPANN to complete a single run may not seem too long, it must be kept in mind that all of the aforementioned variables have to be optimized, so this process should be repeated several times before the most adequate BPANN is finally obtained. All of the above contribute to making the entire development of a GRANN not only simpler but also faster when compared to its backpropagation counterpart.

As mentioned earlier, only the width of the radial basis function (the SPREAD value) has to be optimized when developing a GRANN. Figure 2 depicts the variation of the RMSPD with the logarithm of the SPREAD value in the range between −3.0 and 0 (corresponding to a SPREAD value ranging between 1×10^{-3} and 1.0). It can be seen that the RMSPD varied only slightly below 1×10^{-2}, but rose to high values (>7.2) above the latter. Although a SPREAD value of 1×10^{-3} was chosen on the basis of this study, it was later seen that values between 10^{-3} and 10^{-2} did not affect the performance of the corresponding networks when presented with unknown input data.

When comparing the performance of the various models (see Table 2) it was found that the best result, in terms of the RMSPD, was achieved with the GRANN (0.39), whereas the worst one was obtained with the Lorentzian fit (13.57). Interestingly enough, the regression analyses of the predicted versus nominal concentrations did not reflect the same marked difference in the goodness-of-fit that revealed the RMSPD. Effectively, on the one hand, a statistical analysis of the intercepts and the slopes of the various models showed that there were no reasons to reject the null hypothesis at the 95% confidence level [22]. On the other hand, the coefficient of determination (r^2) in all cases is close to the unity (≥ 0.996). Nevertheless, a visual inspection of the corresponding graphs (see Fig. 3) revealed important deviations of the predicted results for the Lorentzian and Gaussian fits from the ideal line (zero intercept and unity slope) at cadmium concentrations of ≥16.0 μg L^{-1}. This inaccuracy is not observed in other models, such as the GRANN, BPANN, or Boltzmann fit, the last of which is shown in the same figure for comparison purposes. That such deviations occur randomly around the ideal line, at least for the Lorentzian model, may explain the apparent

Table 2 Root mean square of the percentage deviations and regression estimates of predicted versus expected cadmium concentrations for various nonlinear models

Model	RMSPD	Regression analysis	r^2 Value
GRANN	0.39	$[Cd]_{Pred} = [Cd]_{Nom}$	1.0000
Boltzmann	2.55	$[Cd]_{Pred} = 1.000[Cd]_{Nom} - 0.0007$	0.9989
Second-order polynomial	3.04	$[Cd]_{Pred} = 1.001[Cd]_{Nom} - 0.0051$	0.9989
BPANN	4.32	$[Cd]_{Pred} = 1.001[Cd]_{Nom} - 0.0479$	0.9988
Gaussian	6.73	$[Cd]_{Pred} = 1.059[Cd]_{Nom} - 0.1332$	0.9969
Lorentzian	13.57	$[Cd]_{Pred} = 0.997[Cd]_{Nom} - 0.0011$	0.9959

goodness-of-fit of the regression analysis, whereas the absolute magnitude of the deviations may account for the comparatively large value of these models' RMSPDs.

Determination of Cd by GFAAS in a certified reference material

The predicting abilities of the models shown in the preceding section were finally evaluated in the determination of cadmium in the certified reference material (CRM) "Trace Metals in Drinking Water". This reference material was, as stated in the procedure section, prepared at four concentration levels so that the concentration of the first two solutions would lie in the linear portion of the calibration curve, whereas the second two would lie in the non-linear portion. No other reference material with an elevated cadmium concentration was available at the time this research project was under progress, so the ruggedness of the proposed methodology was assessed using only the aforementioned one.

The integrated absorbance recorded for each solution was input into the various models previously evaluated and the concentrations thus predicted were statistically compared to the expected concentrations. It can be seen from the results summarized in Table 3 that good precision is attained in all cases (< 2.00% RSD). The accuracy, on the other hand, is good (i.e., the results are not significantly different ($p \leq 0.05$) [22]) only for the predictions given by the models generated by the backpropagation and the GRANN. Quite contrarily, significant differences at the 95% confidence level were found for the concentrations predicted by all the other models. Careful inspection of Table 3 reveals large differences between cadmium's concentrations predicted by such models and the expected ones, which accounts for the inaccuracy of the models when applied to a more complex specimen. The latter is even more surprising when it is taken into account that the RMSPD for the second-order polynomial and the Boltzmann fits were lower than the corresponding value attained with the BPANN model. From these results it seems reasonable to surmise that the models generated by the ANNs are more robust, that is, the noise in the input variable can be incorporated into the model in a way that greatly reduces the predicted errors. Aside from the accuracy of the results obtained with both neural networks, the possibility mentioned in the preceding lines seems to be supported by the fact that the GRANN model was able to predict the exact concentration of the test solutions, disregarding the dispersion intrinsic to the input variable. This "zero-error" outcome was realized with SPREAD values ranging from 1×10^{-3} to 1×10^{-2}, whereby the model fitness was best (RMSPD ≤ 0.9). It was only above a SPREAD value of 5×10^{-2} that the predicted results statistically differed from the expected values ($p \leq 0.05$), a clear consequence of the deterioration of the models'

Table 3 Determination of Cd in the CRM "Trace Elements in Drinking Water" using different calibration models

Concentration (μg L^{-1})[a]	Model					
	Second-order polynomial	Lorentzian	Gaussian	Boltzmann	BPANN[b]	GRANN[b]
2.00 ± 0.05	2.10 ± 0.03 (1.40)	2.15 ± 0.03 (1.53)	2.15 ± 0.03 (1.45)	2.09 ± 0.03 (1.39)	2.03 ± 0.03 (1.40)	2.00 ± 0.00 (0.00)
4.00 ± 0.08	4.19 ± 0.04 (1.05)	4.41 ± 0.05 (1.04)	4.34 ± 0.05 (1.04)	4.16 ± 0.04 (1.04)	4.08 ± 0.04 (1.10)	4.00 ± 0.00 (0.00)
8.00 ± 0.12	8.02 ± 0.11 (1.41)	8.22 ± 0.11 (1.31)	8.20 ± 0.11 (1.36)	7.98 ± 0.11 (1.42)	7.90 ± 0.12 (1.50)	8.00 ± 0.00 (0.00)
12.00 ± 0.06	12.25 ± 0.07 (0.60)	12.14 ± 0.07 (0.55)	12.34 ± 0.07 (0.58)	12.27 ± 0.08 (0.61)	12.30 ± 0.08 (0.60)	12.00 ± 0.00 (0.00)

The results correspond to the average concentration (μg L^{-1}) ± standard deviation ($N = 5$). Values in parenthesis represent the relative standard deviation
[a] Nominal concentrations of solutions prepared by diluting the CRM "Trace Elements in Drinking Water"
[b] No significant differences ($p \leq 0.05$) between the nominal and the predicted concentrations

goodness-of-fit (RMSPD≥7.2). Such an outstanding predicting performance may suggest that the generalized regression neural network is capable of learning the associations between the independent and dependent variables without being as easily fooled by the naturally occurring statistical variability of the input data as its backpropagation counterpart. The latter may also be an indicator that selection of the training patterns from the whole data space may be less troublesome for the GRANN than for the BPANN.

Conclusions

Cadmium's working calibration range was successfully increased by adequately modeling its nonlinearity by means of a generalized regression and a BPANN. While the BPANN is certainly the most popular variety of neural networks implemented in analytical chemistry applications, the GRANN is more attractive for modeling purposes owing to the speed with which it can be developed. Effectively, only the width of the transfer function has to be determined, and the adjustment of the weights takes place in a single pass. The latter feature makes the GRANN a strong competitor of conventional mathematical fits when modeling non-linear systems, as well as an attractive tool that should be further evaluated for analytical applications. The results presented in this work do not imply that mathematical equations are by any means inadequate for modeling the calibration curves obtained in spectroscopic analysis. What the results do highlight is that the main problem associated with the selection of such models (i.e., the assessment of the regression coefficients and the inaccuracy that may result from this) may be minimized when using ANNs for modeling purposes.

References

1. de Galan L (1987) J Anal At Spectrom 2:89–93
2. Lonardo RF, Yuzefovsky AI, Zhou JX, McCaffrey JT, Michel RG (1996) Spectrochim Acta Part B 51:1309–1323
3. L'vov BV, Polzik LK, Kocharova NV (1992) Spectrochim Acta Part B 47:889–895
4. Vale MGR, Silva MM, Welz B, Nowka R (2002) J Anal At Spectrom 17:38–45
5. Long JR, Gregoriou VG, Gemperline PJ (1990) Anal Chem 62:1791–1797
6. Gemperline PJ, Long JR, Gregoriou VG (1991) Anal Chem 63:2313–2323
7. Sun G, Chen X, Li Q, Wang H, Zhou Y, Hu Z (2000) Fresenius J Anal Chem 367:215–219
8. Hernández-Caraballo EA, Ávila-Gómez RM, Rivas F, Burguera M, Burguera JL (2004) Talanta 63:425–431
9. Zupan J, Gasteiger J (1999) Back-propagation of errors, Chap. 8. In: Neural networks in chemistry and drug design, 2nd edn. Wiley-VCH, Weinheim, pp 125–154
10. Demuth H, Beale M (2000) Radial basis networks. In: Neural network toolbox for use with MATLAB, user's guide version 4, pp 7-1–7-20
11. HGA-700 Graphite furnace operator's manual (1990) Perkin-Elmer, Part No. B017–4145
12. HPS Certified Reference Material "Trace Metals in Drinking Water", Certificate of analysis. High Purity Standards, Charleston
13. Wythoff BJ (1993) Chemom Intell Lab Syst 18:115–155
14. Propagator (1993) Neural network development software, version 1.0 for Windows, ARD Corp., USA
15. Specht DF (1991) IEEE Trans Neural Netw 2:568–576
16. Nadaraya EA (1964) Theory Probab Applic 10:186–190
17. Miller-Ihli NJ, O'Haver TC, Harnly JM (1984) Spectrochim Acta Part B 39:1603–1614
18. Bysouth SR, Tyson JF (1986) J Anal At Spectrom 1:85–87
19. Kim B, Park S (2000) ICASE (The Institute of Control, Automation and Systems Engineers), Korea 2:268–274
20. Hyun BG, Nam K (1995) In: Proceeding of the 1995 IEEE IECON 2:1456–1461
21. Marteau PF, Monbet V (2004) WSEAS Trans Syst 3:346–351
22. Miller JN, Miller JC (2000) Statistics and chemometrics for analytical chemistry, 4th edn. Prentice Hall, Great Britain